

October 1994

Wash. U. HEP/94-63

hep-lat/9411005

Chiral Perturbation Theory and the Quenched Approximation of QCD*

MAARTEN F.L. GOLTERMAN**

*Department of Physics
Washington University
St. Louis, MO 63130, USA*

ABSTRACT: The quenched approximation for QCD is, at present and in the foreseeable future, unavoidable in lattice calculations with realistic choices of the lattice spacing, volume and quark masses. In these lectures, I review the analytic study of the effects of quenching based on chiral perturbation theory. Quenched chiral perturbation theory leads to quantitative insight into the difference between quenched and unquenched QCD, and reveals clearly diseases which plague quenched QCD. A short review of the ideas underlying chiral perturbation theory is included.

* Lectures given at the XXXIV Cracow School of Theoretical Physics, Zakopane, Poland

** e-mail: maarten@aapje.wustl.edu

1. Introduction

The lattice formulation of QCD has proven to be a powerful tool for computing QCD quantities of direct phenomenological interest, such as hadron masses, decay constants, weak matrix elements, the strong coupling constant, *etc.* (For reviews see for instance refs. [1,2], the proceedings of Lattice 93 [3], and the lectures of Rajan Gupta in these proceedings.)

In order to perform such computations numerically, one obviously needs to consider a system with a finite number of degrees of freedom, which is accomplished by putting lattice QCD in a finite box. This box is then hopefully large enough to accommodate the physics one is interested in without serious finite size effects. This leads to the (minimal) requirement that the Compton wavelength of the particles of interest is sufficiently smaller than the linear dimension of the box, *i.e.* the mass has to be large enough for the particles to fit in the box.

In order to have a small enough lattice spacing, small enough masses (in particular for the pion) and a large enough box size, one needs a large number of degrees of freedom in a numerical computation. It turns out that for QCD with realistic choices of the lattice spacing a , volume V and the quark masses (in particular the light quark masses), the presently available computational power is not adequate. The most severe problem comes from the fermion determinant, the logarithm of which is a very nonlocal part of the gluon effective action (specially for light quark masses). This nonlocality slows down currently available algorithms dramatically.

In order to “circumvent” this problem, most numerical computations in lattice QCD have been done in the quenched approximation, in which one simply replaces the fermion determinant by one [4]. This amounts to ignoring all fermion loops which occur in QCD correlation functions (except those put in by hand through the choice of operators on the

external lines). While some handwaving arguments exist as to why this might not be unreasonable, the quenched approximation does introduce an uncontrolled systematic error. Since the effect of a fermion loop is roughly inversely proportional to the fermion mass, this error is expected to be particularly large for quantities involving light quarks. Therefore one might expect that chiral perturbation theory (ChPT) is a useful tool for investigating the difference between quenched and unquenched (“full”) QCD.

In this talk, I will review a systematic approach to the study of the quenched approximation through ChPT [5,6,7,8]. There are two reasons why ChPT is useful in this context:

- It turns out that ChPT can be systematically adapted to describe the low energy sector of quenched QCD [6]. It will therefore give us nontrivial, quantitative information on the difference between quenched and full QCD.
- ChPT describes the approach to the chiral limit, and can be used for extrapolation of numerical results to small masses and large volumes. If these results come from quenched computations, one will of course need a quenched version of ChPT. (For finite volume ChPT, see refs. [9]. For quenched finite volume results, see refs. [6,7].)

In this review, I will concentrate on the first point. First, I will give a short summary of the basic underpinnings of ChPT, in order to make these lectures more or less selfcontained. I will then give an early example of numerical results which can be understood using one loop ChPT. I will then go on to show how ChPT is developed for the quenched approximation, and use it for a quantitative comparison between full and quenched QCD. The quantities that I will discuss are f_K/f_π [6,8,10] and the octet baryon masses [11].

I will then address a number of theoretical problems that arise as a consequence of quenching. That such problems arise is no surprise, as quenching QCD mutilates the theory quite severely. It is however quite instructive to see what the actual consequences are.

2. A review of ChPT

In this section I will summarize the basic ideas of ChPT, which is an efficient way to organize the information we can obtain from the QCD Ward identities for chiral symmetry. A partial list of useful references is [12,13,14]. Let us start with QCD with three flavors. The fermion part of the lagrangian is

$$\mathcal{L}_{\text{QCD}} = \bar{q}_L \not{D} q_L + \bar{q}_R \not{D} q_R + \bar{q}_L M q_R + \bar{q}_R M^\dagger q_L. \quad (1)$$

$q = (u, d, s)$ is a three flavor quark field, and the subscripts L and R denote the left- and righthanded projections $q_{L,R} = \frac{1}{2}(1 \pm \gamma_5)q$. M is the quark mass matrix

$$M = \begin{pmatrix} m_u & 0 & 0 \\ 0 & m_d & 0 \\ 0 & 0 & m_s \end{pmatrix}. \quad (2)$$

For $M = 0$, the lagrangian is invariant under the chiral symmetry group $U(3)_L \times U(3)_R$:

$$q_L \rightarrow U_L q_L, \quad q_R \rightarrow U_R q_R, \quad U_L, U_R \in U(3). \quad (3)$$

Note that formally eq. (1) is invariant if we also let M transform as

$$M \rightarrow U_L M U_R^\dagger. \quad (4)$$

Axial $U(1)$ transformations (*i.e.* $U(1)$ transformations on the fields q_L and q_R for which the phases are not equal) however are not a symmetry of the theory, since they are broken by the axial anomaly. The real symmetry group is therefore $SU(3)_L \times SU(3)_R \times U(1)$ where the $U(1)$ just corresponds to quark number conservation. It is furthermore believed that (still for $M = 0$) this symmetry is spontaneously broken to $SU(3)_V \times U(1)$, where $SU(3)_V$ is the group of transformations for which $U_L = U_R \in SU(3)$. The ensuing eight Goldstone bosons are the mesons $\pi^\pm, \pi^0, K^\pm, K^0, \bar{K}^0$ and η , which transform in the octet representation of $SU(3)$, denoted as the hermitian, traceless 3×3 matrix ϕ :

$$\phi = \begin{pmatrix} \frac{\pi^0}{\sqrt{2}} + \frac{\eta}{\sqrt{6}} & \pi^+ & K^+ \\ \pi^- & -\frac{\pi^0}{\sqrt{2}} + \frac{\eta}{\sqrt{6}} & K^0 \\ K^- & \bar{K}^0 & -\frac{2\eta}{\sqrt{6}} \end{pmatrix}. \quad (5)$$

These mesons acquire a nonzero mass due to the quark mass matrix M , as we will discuss below.

One can now try to describe the physics of hadrons by constructing an effective lagrangian for composite operators with the quantum numbers of these hadrons. Explicitly, the operator $H_{ij} = q_{Li}\bar{q}_{Rj}$ (summed over color and spin indices, i and j are flavor indices) will couple to the Goldstone mesons, and one can introduce other operators for other hadrons, and write down an effective lagrangian of the form

$$\mathcal{L}_{\text{eff}}(H, H^\dagger, \text{baryons}, \dots). \quad (6)$$

This lagrangian, integrated over space-time, should be invariant under $SU(3)_L \times SU(3)_R \times U(1)$ transformations $H \rightarrow U_L H U_R^\dagger$ etc. We can decompose $H = R\Sigma$ with R hermitian and positive, and Σ unitary. The spontaneous symmetry breakdown $SU(3)_L \times SU(3)_R \times U(1) \rightarrow SU(3)_V \times U(1)$ corresponds to R acquiring a nonzero vacuum expectation value $r\mathbf{1}$. Dropping the other fields in \mathcal{L}_{eff} , the effective potential does not depend on Σ , and $\Sigma = \exp(2i\phi/f)$ can therefore be identified with the Goldstone bosons, eq. (5), leading to the nonlinear realization of chiral symmetry [15]. f is a constant with the dimension of a mass. (The overall phase of Σ corresponds to the η' which is not a Goldstone boson due to the anomaly [16,17], and has a mass of order 1 GeV.) The fluctuations of ϕ describe the Goldstone mesons, whereas fluctuations in R around $r\mathbf{1}$ describe other heavy (scalar) mesons (which may or may not exist as narrow resonances in nature).

At low energies (energies below the masses of any non-Goldstone hadrons) the effective lagrangian simplifies to

$$\mathcal{L}_{\text{eff}}(\Sigma, M), \quad (7)$$

which has to be invariant under the transformations

$$\begin{aligned} \Sigma &\rightarrow U_L \Sigma U_R^\dagger, \\ M &\rightarrow U_L M U_R^\dagger. \end{aligned} \quad (8)$$

This follows from the definition of H , which, ignoring fluctuations in R , is $H = r\Sigma$ and from the invariance of the QCD path integral under the transformations eqs. (3, 4). Note that the unbroken symmetry $SU(3)_V$ is linearly realized ($\Sigma \rightarrow V\Sigma V^\dagger$ implies $\phi \rightarrow V\phi V^\dagger$), whereas the broken symmetries are nonlinearly realized.

Let us imagine that we can expand \mathcal{L}_{eff} in terms of derivatives and the quark mass matrix M . To second order in derivatives and linear order in M , (we will call this “ $O(p^2)$ ”) the most general expression is¹

$$\mathcal{L}_{\text{eff}} = \frac{f^2}{8} \text{tr}(\partial_\mu \Sigma \partial_\mu \Sigma^\dagger) - v \text{tr}(M\Sigma^\dagger + M^\dagger \Sigma), \quad (9)$$

where f and v are undetermined constants. Expanding \mathcal{L}_{eff} to quadratic order in the meson field ϕ (eq. (5)) using $\Sigma = 1 + \frac{2i\phi}{f} + \dots$ one will see that the kinetic terms have the standard normalization, and one can read off the tree level meson masses (for simplicity I will choose $m_u = m_d = m$):

$$m_\pi^2 = \frac{8vm}{f^2}, \quad m_K^2 = \frac{4v(m + m_s)}{f^2}, \quad m_\eta^2 = \frac{8v(m + 2m_s)}{3f^2}. \quad (10)$$

We see that the mesons acquire masses proportional to the square root of the quark masses, and in the chiral limit $M \rightarrow 0$ they are massless as they should be. Note that for onshell mesons the combined expansion to second order in derivatives and to first order in M is consistent. Note also that we obtained our first nontrivial result: from eq. (10) it follows that

$$m_\eta^2 = \frac{4}{3}m_K^2 - \frac{1}{3}m_\pi^2, \quad (11)$$

which predicts a value of m_η about 3% too large.

Let us proceed, and calculate scattering amplitudes A to some order in the loop expansion. In order to do this we need to introduce a cutoff Λ . The physical reason for this is that we are now ignoring all the hadronic physics at energies of order the ρ mass and beyond.

¹ We will not need to consider the Wess–Zumino term, see ref. [14] and refs. therein.

We therefore expect that we will have to choose Λ to be of the order of the ρ mass, *i.e.* or order 1 GeV . Using dimensional regularization and power counting one obtains for the contribution of a certain diagram to A [12,13]

$$(2\pi)^4 \delta(\sum_i p_i) f^2 p^2 \left(\frac{p^2}{(4\pi f)^2} \right)^N \left(\frac{1}{f} \right)^E F(p^2/\Lambda^2). \quad (12)$$

We identified $\Lambda \approx 4\pi f$, which is of order 1 GeV (f will turn out to be the pion decay constant, as we will see in a moment) [13]. Here p_i stands for external momenta, and p^2 denotes the square of any linear combination of these; it can also be a Goldstone meson mass squared. E is the number of external lines, and

$$N = \sum_d \frac{1}{2} (d-2) V_d + L, \quad (13)$$

where L is the number of loops and V_d is the number of vertices with d derivatives (or $d/2$ powers of M , or any combination in between). F is a function containing logarithmic divergences in Λ arising from diagrams with loops.

From eq. (12) we can draw the following conclusions. An amplitude A can be calculated as a series expansion in $p^2/(4\pi f)^2$ if \vec{p}^2 and m_{meson}^2 are much smaller than $\Lambda^2 = (4\pi f)^2$. In eq. (9) we only allowed $O(p^2)$ terms, but we could have allowed higher order terms. From eq. (12) we see that treelevel contributions from $O(p^4)$ terms come in at the same order as one loop terms from the $O(p^2)$ lagrangian eq. (9): $N = 1$ corresponds to $L = 1$ and $V_4 = 0$ or $L = 0$ and $V_4 = 1$. Therefore the $O(p^4)$ terms act as counterterms at the one loop level, and in fact need to be added at this order in order to absorb the cutoff dependence (*cf.* F in eq. (12)). A change in the choice of Λ can be absorbed by a shift in these counterterms. These conclusions generalize systematically to higher loops ($L > 1$). A very important conclusion of this analysis is that at any given order in $p^2/(4\pi f)^2$ we only need a finite number of counterterms, and therefore the theory is predictive. Furthermore, the nonanalytic terms at L loops (contained in F) are determined by the $O(p^{d=2L})$ lagrangian (*i.e.* by diagrams with $V_d = 0$ for $d > 2L$).

As an example I will now discuss the decay constants f_π and f_K . First consider $N = 0$, so that the $O(p^2)$ lagrangian at tree level is sufficient. The pion decay constant f_π in QCD is defined by the matrix element of the lefthanded Noether current $j_{L\mu} = \bar{d}_L \gamma_\mu u_L$ between a one pion state and the vacuum:

$$\langle 0 | j_{L\mu}(x) | \pi^+(p) \rangle = \frac{i}{2} p_\mu f_\pi e^{-ipx}. \quad (14)$$

(It is this current which couples to the electroweak W bosons, through which the pion decays into a pair of leptons.) In ChPT this Noether current can be determined from eq. (9), leading to

$$j_{L\mu} = \frac{if^2}{4} \text{tr}(T^+ \partial_\mu \Sigma \Sigma^\dagger) = -\frac{f}{2} \partial_\mu \pi^+ + \dots, \quad (15)$$

where T^+ is the appropriate $SU(3)$ generator, and hence

$$\langle 0 | j_{L\mu}(x) | \pi^+(p) \rangle = \frac{i}{2} p_\mu f e^{-ipx}. \quad (16)$$

We conclude that at this order $f_\pi = f (= 132 \text{ GeV})$ which determines the constant f . A similar calculation leads to

$$f_K = f = f_\pi, \quad (17)$$

which is a prediction, off by 22%.

We see that the relation between f_K and f_π is consistent with $SU(3)_V$ symmetry. The $SU(3)_V$ breaking introduced by the quark masses shows up at the one loop order ($N = 1$). From ref. [14]

$$\frac{f_K}{f_\pi} = 1 + \frac{5}{4} \frac{m_\pi^2}{16\pi^2 f_\pi^2} \log\left(\frac{m_\pi^2}{\Lambda^2}\right) - \frac{1}{2} \frac{m_K^2}{16\pi^2 f_\pi^2} \log\left(\frac{m_K^2}{\Lambda^2}\right) - \frac{3}{4} \frac{m_\eta^2}{16\pi^2 f_\pi^2} \log\left(\frac{m_\eta^2}{\Lambda^2}\right) + \frac{m_K^2 - m_\pi^2}{16\pi^2 f_\pi^2} L, \quad (18)$$

where L is a linear combination of coefficients of $O(p^4)$ terms in the effective lagrangian [14]. With $\Lambda = 1 \text{ GeV}$ the experimental value $f_K/f_\pi = 1.22$ can be reproduced with $L = 1.1$. Notice that the coefficient of $\log(1/\Lambda^2)$ is proportional to $m_K^2 - m_\pi^2$, so a change

in the cutoff can be absorbed by a shift in L . We also see that the expansion parameters are

$$\frac{m_\pi^2}{16\pi^2 f_\pi^2} \approx 0.007, \quad \frac{m_K^2}{16\pi^2 f_\pi^2} \approx 0.09, \quad (19)$$

which are small. In contrast, $\frac{m_D^2}{16\pi^2 f_\pi^2} \approx 1.3$, and hence the charm quark mass cannot be considered as small in the sense of chiral perturbation theory.

An equation like eq. (18) can be used in two ways. First, we can determine L from the experimental values for f_K and f_π (fixing Λ at some value of order 1 GeV). This can then be used to predict other quantities, like f_η [14]. Second, eq. (18) can be used to fit results from numerical computations. Since these usually are performed at relatively large values of the quark mass (and hence the Goldstone meson masses), we can then employ results from ChPT to extrapolate to the physical values of quark masses.

3. An example: B_K

In this section, I would like to give an example of the definition and use of an electroweak operator in ChPT (for much more detail see *e.g.* refs. [13,18] and refs. therein). The kaon B parameter, B_K , which determines the strength of $K^0 - \bar{K}^0$ mixing, is defined as

$$\frac{8}{3} f_K^2 m_K^2 B_K = \langle \bar{K}^0 | \mathcal{O}_K | K^0 \rangle, \quad (20)$$

with

$$\mathcal{O}_K = (\bar{s}_L \gamma_\mu d_L) (\bar{s}_L \gamma_\mu d_L). \quad (21)$$

\mathcal{O}_K transforms as a component of the $(27, 1)$ representation of $SU(3)_L \times SU(3)_R$. This symmetry property can be used to construct a corresponding operator in ChPT, which to $\mathcal{O}(p^2)$ is uniquely given by

$$\mathcal{O}_K^{\text{ChPT}} = \frac{1}{3} B f^4 (\partial_\mu \Sigma \Sigma^\dagger)_{ds} (\partial_\mu \Sigma \Sigma^\dagger)_{ds}. \quad (22)$$

(Note that in both QCD and ChPT this operator is the product of two lefthanded currents.) The coefficient B is undetermined, and is therefore another free parameter in ChPT, like f and v . To one loop order, we may calculate B_K from eqs. (20, 22), and we obtain (for degenerate quark masses, *cf.* ref. [19,7] for the nondegenerate case)

$$B_K = B \left(1 - 6 \frac{m_\pi^2}{16\pi^2 f_\pi^2} \log \frac{m_\pi^2}{\Lambda^2} \right) + O(p^4) \text{ contributions.} \quad (23)$$

In ref. [7], besides B_K , a different quantity B_V was studied, which, as we will see, has chiral one loop corrections larger than B_K has. For all details not discussed here I refer to ref. [7]. The quantity B_V is defined from

$$\frac{4}{3} f_K^2 m_K^2 B_V = \langle \overline{K}'^0 | [(\overline{s}'_a \gamma_\mu d'_b)(\overline{s}_b \gamma_\mu d_a) + (\overline{s}'_a \gamma_\mu d'_a)(\overline{s}_b \gamma_\mu d_b)] | K^0 \rangle, \quad (24)$$

where a and b are color indices. d' and s' are new flavors of quarks, and \overline{K}'^0 is a kaon built out of those. This is a technical trick to reduce the number of Wick contractions on eq. (24) to one. All quark masses are chosen equal. Note that I use a normalization for the meson decay constants which is different from that used in ref. [7]. With B_A defined similarly with $\gamma_\mu \rightarrow \gamma_\mu \gamma_5$ we have

$$B_K = B_V + B_A. \quad (25)$$

One now can calculate B_V to one loop in ChPT, where in this special case (with degenerate quark masses) one can argue that the result is the same in the quenched and unquenched theories. The result is

$$B_V = \frac{1}{2} B_K - \frac{3}{4} \beta \frac{v^2}{m_K^2} I_2(m_K^2) - \frac{3}{8} \delta - \frac{3}{8} \gamma I_2(m_K^2) + O(m_K^2), \quad (26)$$

where

$$I_2(m^2) = \frac{m^2}{f^2} \int \frac{d^4 p}{(2\pi)^4} \frac{1}{(p^2 + m^2)^2}. \quad (27)$$

β , γ and δ are coefficients of operators in ChPT which arise in the calculation of B_V to one loop (contrary to the case of B_K there is more than one [7]). B_A is given by the same expression with opposite signs for β , γ and δ .

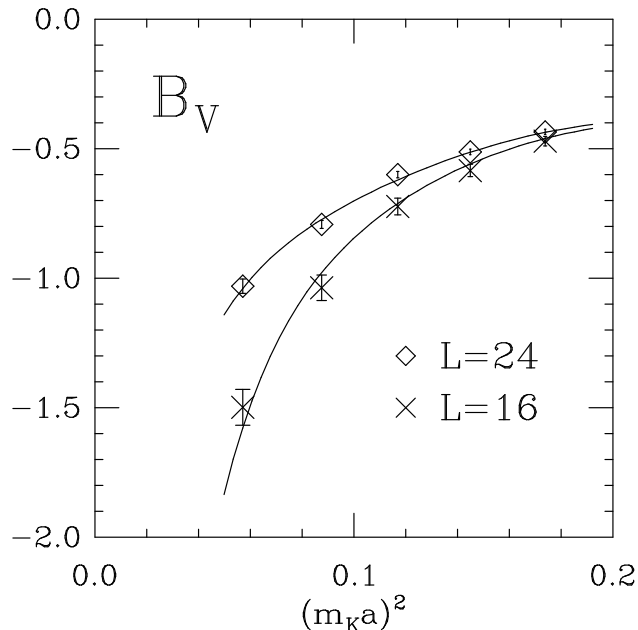


Figure 1. Results for B_V versus m_π^2 ($= m_K^2$) in lattice units (from ref. [7]).

From eq. (26) we see why it is interesting to consider B_V . Unlike in B_K there appears an “enhanced” chiral logarithm in B_V [20] — the second term on the righthand side of eq. (26). The extra factor m_K^2 in the denominator, if small enough, will enhance the size of this correction. If we repeat the calculation in a finite volume $V = L^3$, B_V becomes L dependent because the spatial part of the integral I_2 now has to be replaced by a one loop momentum sum over momenta $\vec{p} = 2\pi\vec{n}/L$ with $\vec{n} \in \mathbb{Z}^3$ (with periodic boundary conditions). Volume dependence of this nature has actually been seen in numerical results. Fig. 1 is from ref. [7]. In this graph the points represent quenched numerical results. The solid lines show the result of a fit of the parameters $\frac{1}{2}B_K - \frac{3}{8}\delta$, β , and γ (for a precise explanation of the fit see again ref. [7]). The graph shows that the numerical results are within errors consistent with one loop ChPT. Because the enhanced logarithms do not appear in B_K itself, one loop effects in this case are too small to be seen with the current statistical errors present in the numerical results for B_K .

This concludes our first example of a confrontation of one loop ChPT with numerical

computations. In this special case, the results from ChPT are unchanged by the effects of quenching. This is in general not true, and a systematic way of changing ChPT to correspond to the quenched approximation needs to be developed. I will do this in the next section, and then return to other, more recent, examples.

4. Systematic ChPT for quenched QCD

In this section I will outline the construction of a chiral effective action for the Goldstone boson sector of quenched QCD [6]. I will first introduce the formalism, and then show how it works in some examples. For early ideas on quenched ChPT, see ref. [21,5].

We will start from a lagrangian definition of euclidean quenched QCD. (We will restrict ourselves entirely to the euclidean theory which can be defined by a pathintegral. Hamiltonian quenched QCD presumably does not exist.) To the usual QCD lagrangian with three flavors of quarks q_a , $a = u, d, s$, we add three ghost quarks \tilde{q}_a with exactly the same quantum numbers and masses m_a , but with opposite, bosonic, statistics [21]:

$$\mathcal{L}_{\text{quarks}} = \sum_a \bar{q}_a (\not{D} + m_a) q_a + \sum_a \bar{\tilde{q}}_a (\not{D} + m_a) \tilde{q}_a, \quad (28)$$

where \not{D} is the covariant derivative coupling the quarks and ghost quarks to the gluon field. The gluon effective action produced by integrating over the quark- and ghost quarkfields vanishes, since the fermion determinant of the quark sector is exactly cancelled by that of the ghost sector. Note that the ghost quarks violate the spin-statistics theorem. Eq. (28) is the lagrangian definition of quenched QCD.

We will now assume that mesons are formed as (ghost) quark - (ghost) antiquark pairs just like in ordinary QCD. This is basically equivalent to the notion that it is the dynamics of the gluons which leads to confinement and chiral symmetry breaking. The Goldstone particle spectrum of quenched QCD will then contain not only $q\bar{q}$, but also $\tilde{q}\bar{\tilde{q}}$, $q\bar{\tilde{q}}$ and $\tilde{q}q$

bound states. We will denote this 36-plet by

$$\Phi \equiv \begin{pmatrix} \phi & \chi^\dagger \\ \chi & \phi \end{pmatrix} \sim \begin{pmatrix} q\bar{q} & q\bar{\tilde{q}} \\ \tilde{q}\bar{q} & \tilde{q}\bar{\tilde{q}} \end{pmatrix}. \quad (29)$$

Note that the fields χ and χ^\dagger describe Goldstone fermions.

The quenched QCD lagrangian eq. (28) with zero quark masses has a much larger symmetry group than the usual $U(3)_L \times U(3)_R$ chiral group; it is invariant under the graded group $U(3|3)_L \times U(3|3)_R$ [6], where $U(3|3)$ is a graded version of $U(6)$ since it mixes the fermion and boson fields q and \tilde{q} . Writing an element U of $U(3|3)$ in block form as

$$U = \begin{pmatrix} A & C \\ D & B \end{pmatrix}, \quad (30)$$

the 3×3 matrices A and B consist of commuting numbers, while the 3×3 matrices C and D consist of anticommuting numbers.

We can now construct a low energy effective action for the Goldstone modes along the usual lines. We introduce the unitary field

$$\Sigma = \exp(2i\Phi/f), \quad (31)$$

which transforms as $\Sigma \rightarrow U_L \Sigma U_R^\dagger$ with U_L and U_R elements of $U(3|3)$. Because we are dealing here with a graded group, in order to build invariants, we need to use the supertrace *str* and the superdeterminant *sdet* instead of the normal trace and determinant, with [22]

$$\begin{aligned} \text{str}(U) &= \text{tr}(A) - \text{tr}(B), \\ \text{sdet}(U) &= \exp(\text{str} \log(U)) = \det(A - CB^{-1}D)/\det(B). \end{aligned} \quad (32)$$

As one can easily verify, it is this definition of the supertrace that respects the cyclic property. To lowest order in the derivative expansion, and to lowest order in the quark masses, the chiral effective lagrangian consistent with our graded symmetry group is

$$\mathcal{L}_0 = \frac{f^2}{8} \text{str}(\partial_\mu \Sigma \partial_\mu \Sigma^\dagger) - v \text{str}(\mathcal{M}\Sigma + \mathcal{M}\Sigma^\dagger), \quad (33)$$

where \mathcal{M} is the quark mass matrix

$$\mathcal{M} = \begin{pmatrix} M & 0 \\ 0 & M \end{pmatrix}, \quad M = \begin{pmatrix} m_u & 0 & 0 \\ 0 & m_d & 0 \\ 0 & 0 & m_s \end{pmatrix}. \quad (34)$$

As before, f and v are bare coupling constants which are not yet determined at this stage.

The symmetry group is broken by the anomaly to the smaller group $[SU(3|3)_L \times SU(3|3)_R] \circledast U(1)$ (the semidirect product arises as a consequence of the graded nature of the groups involved; the details are irrelevant for this talk). $SU(3|3)$ consists of all elements $U \in U(3|3)$ with $sdet(U) = 1$. The anomalous field is $\Phi_0 = (\eta' - \tilde{\eta}')/\sqrt{2}$, where the relative minus sign comes from the fact that in order to get a nonvanishing triangle diagram, one needs to choose opposite explicit signs for the quark and ghost quark loops, due to the different statistics of these fields. η' is the field describing the normal η' particle, while $\tilde{\eta}'$ is the ghost η' consisting of ghost quarks and ghost antiquarks. We will call the field Φ_0 the super- η' field. The field $\Phi_0 \propto str \log \Sigma = \log sdet \Sigma$ is invariant under the smaller symmetry group, and we should include arbitrary functions of this field in our effective lagrangian. In analogy to ref. [14], the correct chiral effective lagrangian is

$$\begin{aligned} \mathcal{L} = & V_1(\Phi_0) str(\partial_\mu \Sigma \partial_\mu \Sigma^\dagger) - V_2(\Phi_0) str(\mathcal{M} \Sigma + \mathcal{M} \Sigma^\dagger) \\ & + V_0(\Phi_0) + V_5(\Phi_0) (\partial_\mu \Phi_0)^2, \end{aligned} \quad (35)$$

where the function multiplying $i str(\mathcal{M} \Sigma - \mathcal{M} \Sigma^\dagger)$ can be chosen equal to zero after a field redefinition. This lagrangian describes quenched ChPT systematically, as we will show now with a few examples.

For our first example, let us isolate just the quadratic terms for the fields η' and $\tilde{\eta}'$, choosing degenerate quark masses for simplicity. We expand

$$\begin{aligned} V_1(\Phi_0) &= \frac{f^2}{8} + \dots, \\ V_2(\Phi_0) &= v + \dots, \\ V_0(\Phi_0) &= \text{constant} + \mu^2 \Phi_0^2 + \dots, \\ V_5(\Phi_0) &= \alpha + \dots, \end{aligned} \quad (36)$$

and obtain

$$\begin{aligned} \mathcal{L}(\eta', \tilde{\eta}') = & \frac{1}{2}(\partial_\mu \eta')^2 - \frac{1}{2}(\partial_\mu \tilde{\eta}')^2 + \frac{1}{2}\alpha(\partial_\mu \eta' - \partial_\mu \tilde{\eta}')^2 \\ & + \frac{1}{2}m_\pi^2(\eta')^2 - \frac{1}{2}m_\pi^2(\tilde{\eta}')^2 + \frac{1}{2}\mu^2(\eta' - \tilde{\eta}')^2 + \dots, \end{aligned} \quad (37)$$

where $m_\pi^2 = 8mv/f^2$. The relative minus signs between the η' and $\tilde{\eta}'$ terms in eq. (37) come from the supertraces in eq. (35), and are related to the graded nature of the chiral symmetry group of quenched QCD.

The inverse propagator in momentum space,

$$(p^2 + m_\pi^2) \begin{pmatrix} 1 & 0 \\ 0 & -1 \end{pmatrix} + (\mu^2 + \alpha p^2) \begin{pmatrix} 1 & -1 \\ -1 & 1 \end{pmatrix}, \quad (38)$$

clearly cannot be diagonalized in a p independent way, which is quite different from what one would expect from a normal field theory! Treating the $\mu^2 + \alpha p^2$ term as a twopoint vertex, one can easily show that the repetition of this vertex on one meson line vanishes, due to the fact that the propagator matrix $\begin{pmatrix} 1 & 0 \\ 0 & -1 \end{pmatrix}$ multiplied on both sides by the vertex matrix $\begin{pmatrix} 1 & -1 \\ -1 & 1 \end{pmatrix}$ gives zero. This result coincides exactly with what one would expect from the quark flow picture for η' propagation, as depicted in fig. 2. The straight-through and double hairpin contributions do not contain any virtual quark loops, and are therefore present in the quenched approximation. All other contributions should vanish because they do contain virtual quark loops, and this is exactly what happens as a consequence of the (admittedly strange) Feynman rules for the propagator in the $\eta' - \tilde{\eta}'$ sector! This propagator is given by the inverse of eq. (38) and reads

$$\frac{1}{p^2 + m_\pi^2} \begin{pmatrix} 1 & 0 \\ 0 & -1 \end{pmatrix} - \frac{\mu^2 + \alpha p^2}{(p^2 + m_\pi^2)^2} \begin{pmatrix} 1 & 1 \\ 1 & 1 \end{pmatrix}, \quad (39)$$

in which the two terms correspond to the two first diagrams in fig. 2.

Figure 2. *Quark flow diagrams for the η' propagator in full QCD.*

From eq. (39) we learn several things. First, because μ^2 , which in full ChPT would correspond to the singlet part of the η' mass, appears in the numerator, we need to keep the η' (and its ghost partner) in quenched ChPT: it cannot be decoupled by taking μ^2 large. Second, this “propagator” is definitely sick, due to the double pole term. It should be stressed here that this double pole term is an unescapable consequence of quenched QCD, and does not result from our way of setting up chiral perturbation theory. In the case of nondegenerate quark masses, this double pole also shows up in the π^0 and η propagators, due to mixing with the η' . I will return to these strange properties of quenched QCD in section 6.

Figure 3. *One loop pion selfenergy in quenched ChPT.*

As a second example, we will consider the (charged) pion selfenergy at one loop, again with degenerate quark masses. I will set $\alpha = 0$ for simplicity. At one loop, the pion selfenergy only contains tadpoles, with either ϕ or χ lines (*cf.* eq. (29)) on the loop. Also, on the ϕ loop, one can have an arbitrary number of insertions of the vertex μ^2 if the internal ϕ line is an $SU(3)$ singlet. These various contributions are drawn in fig. 3, where a solid line denotes a ϕ line, a dashed line denotes a χ line, and a cross denotes a μ^2 vertex. One finds that the diagrams with the ϕ and χ lines on the loop without any crosses cancel, and then,

of course, that the diagrams with more than one cross vanish, using our earlier result for the $\eta'-\tilde{\eta}'$ propagator. We are left with only one term, and the result is

$$\Sigma_\pi(p) = \frac{2m_\pi^2}{f^2} \frac{\mu^2}{3} \int \frac{d^4k}{(2\pi)^4} \frac{1}{(k^2 + m_\pi^2)^2}. \quad (40)$$

The pion selfenergy is logarithmically divergent, but this nonanalytic term is completely different from those that arise in the unquenched theory, as it is proportional to μ^2 . One can easily convince oneself that the diagrams in fig. 3 which cancel or vanish correspond to diagrams with virtual quark or ghost quark loops in the quark flow picture. (For early discussions of the quenched pion selfenergy in the quark flow picture, see refs. [21,5].)

Before I go on to look at some quantitative results, I would like to discuss one aspect of the chiral expansion in quenched ChPT. The chiral expansion is basically an expansion in the pion mass (see *e.g.* ref. [12]). However, as we have argued above, in quenched ChPT there is unavoidably another mass scale, namely the singlet part of the η' mass, μ^2 . For our expansion to be systematic as an expansion in the pion mass, we would have to sum up all orders in μ^2 , at a fixed order in the pion mass. This is clearly a formidable task. In order to avoid this complication in a systematic way, we can think of $\mu^2/3$ (which turns out to be the natural parameter as it appears in the chiral expansion) as an independent small parameter. To check whether this makes any sense, one may note that from the experimental value of the η' mass one obtains a value $\mu^2/3 \approx (500 \text{ MeV})^2$, which is roughly equal to the kaon mass squared, m_K^2 . Of course, for quenched QCD the parameter μ^2 need not have the same value, after all quenched QCD is a different theory. A lattice computation of this parameter [23] gives $\mu_{\text{quenched}}^2/\mu_{\text{full}}^2 \approx 0.75$. (α can be estimated from $\eta-\eta'$ mixing, and is very small.) Finally, one may also note that both μ^2 and α are of order $1/N_c$, where N_c is the number of colors [17]. I will return to this point in section 6.

5. Quantitative comparison of quenched and full ChPT

Let us first consider the quenched result for the ratio of the kaon and pion decay constants f_K and f_π [6,8]. I will set $\alpha = 0$ and take $m_u = m_d \equiv m$:

$$\left(\frac{f_K}{f_\pi}\right)_{\text{quenched}}^{1\text{-loop}} = 1 + \frac{\mu^2/3}{16\pi^2 f_\pi^2} \left[\frac{m_K^2}{2(m_K^2 - m_\pi^2)} \log\left(\frac{2m_K^2}{m_\pi^2} - 1\right) - 1 \right] + \frac{m_K^2 - m_\pi^2}{16\pi^2 f_\pi^2} \hat{L}. \quad (41)$$

\hat{L} is again a certain combination of $O(p^4)$ couplings of the quenched chiral lagrangian, which does not have to be equal to L in eq. (18), since it comes from a different theory (quenched QCD). (For example, L is cutoff dependent, while \hat{L} is not.) Because of this, the result eq. (41) is not directly comparable to the equivalent result for the full theory. In other words, in order to compare quenched and full QCD, we have to consider quantities which are independent of the bare parameters of the effective action. (Alternatively, we would need to extract the values of the bare parameters from some independent measurement or lattice computation, in this case, we would need independent determinations of L in both quenched and full QCD.) In the full theory, $(f_\eta f_\pi^{1/3})/f_K^{4/3}$ is such a quantity [14], but in the quenched theory this quantity is not well defined, due to the double poles which occur in the propagators of neutral mesons.

We will therefore choose to consider a slightly different theory, in which sufficiently many charged (*i.e.* off-diagonal) mesons are present [8]. This theory is a theory with two light quarks $m_u = m_d = m$ and two heavy quarks $m_s = m_{s'} = m'$. This theory contains a $u\bar{d}$ pion π , an $s'\bar{s}$ pion π' and a $u\bar{s}$ kaon K , with (tree level) mass relation

$$m_K^2 = \frac{1}{2}(m_\pi^2 + m_{\pi'}^2). \quad (42)$$

One can show that the ratio $f_K/\sqrt{f_\pi f_{\pi'}}$ is independent of the low energy constants L . For the quenched theory we find

$$\left(\frac{f_K}{\sqrt{f_\pi f_{\pi'}}}\right)_{\text{quenched}}^{1\text{-loop}} = 1 + \frac{\mu^2/3}{16\pi^2 f_\pi^2} \left[\frac{m_\pi^2 + m_{\pi'}^2}{2(m_{\pi'}^2 - m_\pi^2)} \log\left(\frac{m_{\pi'}^2}{m_\pi^2}\right) - 1 \right], \quad (43)$$

whereas in the full theory

$$\left(\frac{f_K}{\sqrt{f_\pi f_{\pi'}}}\right)_{\text{full}}^{1\text{-loop}} = 1 - \frac{1}{64\pi^2 f_\pi^2} \left[m_\pi^2 \log\left(\frac{m_K^2}{m_\pi^2}\right) + m_{\pi'}^2 \log\left(\frac{m_K^2}{m_{\pi'}^2}\right) \right]. \quad (44)$$

Note again that the logarithms in the quenched and unquenched expressions are completely different in origin.

We may now compare these two expressions using “real world” data, where we’ll determine the value of the π' mass from the mass relation eq. (42). With $m_\pi = 140 \text{ MeV}$, $m_K = 494 \text{ MeV}$ and $\mu^2/3 = 0.75 \times (500 \text{ MeV})^2$ we find

$$\begin{aligned} \left(\frac{f_K}{\sqrt{f_\pi f_{\pi'}}}\right)_{\text{quenched}}^{1\text{-loop}} &= 1.049, \\ \left(\frac{f_K}{\sqrt{f_\pi f_{\pi'}}}\right)_{\text{full}}^{1\text{-loop}} &= 1.023, \end{aligned} \quad (45)$$

a difference of 3%. If we choose $\mu^2/3 = (500 \text{ MeV})^2$, we find a difference of about 4%. This difference is small. Note however, that this is due to the fact that for this particular ratio, ChPT seems to work very well, both for the full and the quenched theories. If one only considers the size of the one loop corrections (the numbers behind the decimal point), the quenched and full results are very different. It is also possible, and in fact not unlikely, that part of the difference between the full and quenched theory gets “washed out” by the fact that we are considering a “ratio of ratios”. It follows that the relative difference is a lower bound on the difference between the quenched and full values of the decay constants. For another quantity for which the difference between quenched and full ChPT has been calculated, see ref. [8].

Recently, numerical results for quenched f_K/f_π have become available which are precise enough to make a comparison with eq. (43) interesting. These results are shown in fig. 4 [10], in which the solid line depicts a fit of eq. (43) to the numerical results. The quantity X is defined as

$$X = \frac{m_\pi^2 + m_{\pi'}^2}{2(m_{\pi'}^2 - m_\pi^2)} \log\left(\frac{m_{\pi'}^2}{m_\pi^2}\right) - 1, \quad (46)$$

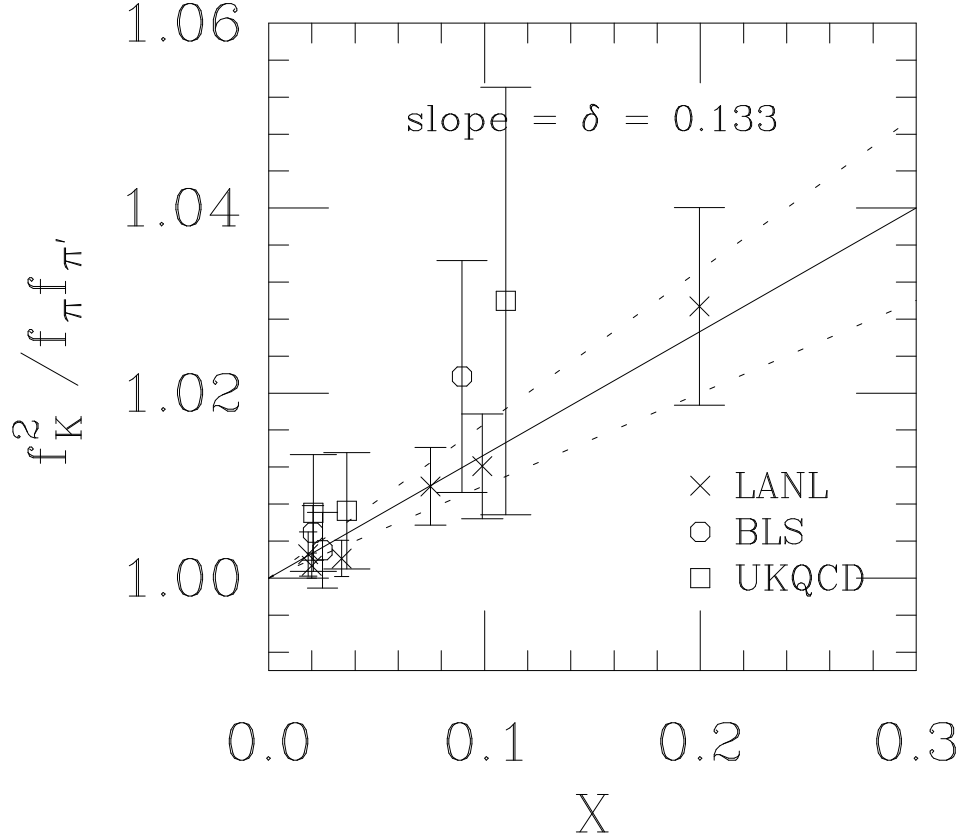


Figure 4. $f_K^2/(f_\pi f_{\pi'})$ versus X (see text for explanation) (adapted from ref. [10]).

and what was fitted is

$$\frac{f_K^2}{f_\pi f_{\pi'}} = 1 + \delta X, \quad (47)$$

with

$$\delta = \frac{\mu^3/3}{8\pi^2 f_\pi^2}. \quad (48)$$

The solid line corresponds to $\delta = 0.133$, and the dashed lines correspond to a variation of ± 0.033 in this value for δ . We expect $\delta = 0.137\text{--}0.182$ from eq. (48) for $\mu^2/3 = (0.75\text{--}1) \times (500 \text{ GeV})^2$. If one plots the same quantity using eq. (44) instead of eq. (43), the results look much less convincing, however, the errors in the numerical results are still quite large. At this stage one can conclude that numerical results are consistent with one

loop quenched ChPT. It would be interesting to have numerical results with smaller errors. For more detail, see ref. [10].

Next, I will review some work on baryons in quenched ChPT by Labrenz and Sharpe [11]. They calculated the one loop corrections to the octet baryon mass coming from the cloud of Goldstone mesons. They employed an effective lagrangian for quenched heavy baryon ChPT, constructed using the same techniques as described in section 4. In the case of degenerate quark masses, the result for the nucleon mass is

$$m_N = \bar{m} - \frac{3\pi}{2}(D - 3F)^2 \frac{\mu^2/3}{8\pi^2 f_\pi^2} m_\pi + 2(b_D - 3b_F)m_\pi^2 + \left[\frac{2}{3}(D - 3F)(2D + 3\gamma) + \frac{5}{6}\alpha(D - 3F)^2 \right] \frac{m_\pi^3}{8\pi f_\pi^2}. \quad (49)$$

In this equation, \bar{m} , D , F , b_D , b_F and γ are bare parameters which occur in the baryon effective action. \bar{m} is the bare “average” octet mass, D and F are the well known baryon-meson couplings, b_D and b_F are low energy constants which arise as a consequence of renormalization (see for instance refs. [24,25]). γ is a new coupling which occurs because of the unavoidable presence of the super- η' in the quenched approximation. The term proportional to μ^2 comes from a diagram with a cross on the ϕ internal line, *i.e.* an insertion of the μ^2 twopoint vertex. Note that in this case there are also one loop corrections not involving μ^2 which survive the quenched approximation, in contrast to the pion selfenergy, eq. (40), or f_K/f_π , eq. (41). The authors of ref. [11] then calculated the coefficients using full QCD values for the various parameters (from ref. [25]). With $\alpha = 0$ and $\gamma = 0$ ($\gamma = 0$ is consistent with available information, which however is limited [26]), they obtained

$$m_N = 0.97 - 0.5 \frac{\delta}{0.2} m_\pi + 3.4 m_\pi^2 - 1.5 m_\pi^3, \quad (50)$$

with δ as in eq. (48) and $\delta \approx 0.2$ for the full theory.

In ref. [11], eq. (49) was also compared to recent numerical results from ref. [27]. These data are presented in fig. 5, where the scale $a^{-1} = 1.63 \text{ GeV}$ is set by f_π [11]. If one

calculates the coefficients in eq. (49) by “fitting” the four data points, one finds

$$m_N = 0.96 - 1.0m_\pi + 3.6m_\pi^2 - 2.0m_\pi^3. \quad (51)$$

This is only four data points for four parameters, and the “fit” is very sensitive to for instance an additional m_π^4 term. Nevertheless, from the agreement between eq. (50) and eq. (51) it appears that it is reasonable to apply ChPT to the results of ref. [27]. Note that the individual terms in eq. (50) are quite large for the two higher pion masses in fig. 5 (this is not unlike the case of unquenched ChPT). From fig. 5 it is also clear that $(\overline{m}/f_\pi)_{\text{quenched}} \neq (\overline{m}/f_\pi)_{\text{full}}$ because of the term linear in eq. (49), which is absent in full ChPT.

Labrenz and Sharpe then went on to consider octet mass splittings. In order to remove effects which can be accomodated by a change of scale, they calculated the ratios

$$R_{ij} = \frac{m_i}{m_j}, \quad i, j = N, \Lambda, \Sigma, \Xi \quad (52)$$

in quenched ChPT, and compared these with similar ratios obtained from ref. [25]. They assumed that all bare parameters in the equations for the octet masses (for explicit expressions, see their paper) are equal in the full and quenched theory, and then calculated the ratios

$$r_{ij} = \frac{R_{ij}^{\text{quenched}}}{R_{ij}^{\text{full}}}. \quad (53)$$

With the assumption that the bare parameters of the quenched and full theories are equal, b_D and b_F drop out of the ratios, and with $\gamma = 0$, $\alpha = 0$ and D and F equal to their full QCD values, they obtain

$$\begin{aligned} r_{\Sigma N} &= 1 + 0.19(\delta/0.2) + 0.13 = 1.31[1.27] \quad \text{for } \delta = 0.2[0.15], \\ r_{\Xi N} &= 1 - 0.46(\delta/0.2) + 0.43 = 0.97[1.09] \quad \text{for } \delta = 0.2[0.15], \\ r_{\Lambda N} &= 1 - 0.39(\delta/0.2) + 0.26 = 0.87[0.97] \quad \text{for } \delta = 0.2[0.15]. \end{aligned} \quad (54)$$

(The choice $\delta = 0.15$ corresponds roughly to the value reported in ref. [23].)

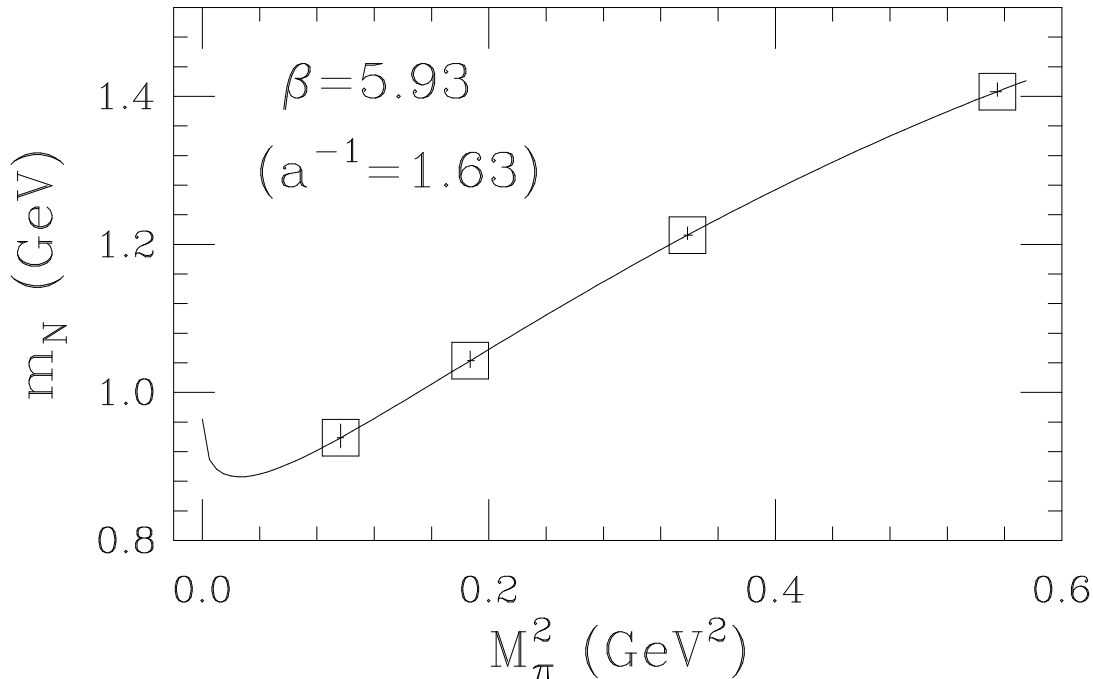


Figure 5. *The nucleon mass from the lattice [27] (copied from ref. [11]). The curve is from a fit to the form $m_N = \bar{m} + am_\pi + bm_\pi^2 + cm_\pi^3$.*

From this, one would conclude that one can expect errors from quenching of at least 20% in the octet splittings. These differences between the quenched and full theories cannot be compensated for by a change in scale between quenched and full QCD.

At this point I would like to comment on the above mentioned assumption that was used in order to obtain eq. (54). Let us consider in particular the parameters b_D and b_F . They correspond to higher derivative terms in the baryon-meson effective action, and are needed in order to absorb the UV divergences which arise at one loop in ChPT. Since the size of these divergences is in principle different between the full and quenched theories, one expects that $b_{D,\text{quenched}}$ and $b_{F,\text{quenched}}$ can be different from $b_{D,\text{full}}$ and $b_{F,\text{full}}$. If we

want to proceed without assuming that the quenched and full b 's are equal, we have to consider ratios of quantities independent of the parameters b_D and b_F . The situation is essentially the same as in the case of f_K/f_π . From the available results [11], only one ratio independent of b_D and b_F can be formed:

$$Y = \frac{m_\Sigma m_\Lambda^3}{m_N^2 m_\Xi^2}. \quad (55)$$

If we expand Y in the Goldstone meson masses using ChPT, $Y - 1$ measures the deviation from the Gell-Mann–Okubo formula (*cf.* ref. [25] for the full theory).

Setting $m_\pi = 0$ keeping only m_K as in ref. [11], one finds

$$\begin{aligned} Y_{\text{quenched}} &= 1 - 1.1046 \frac{m_K^3}{8\pi\bar{m}f_\pi^2} (D^2 - 3F^2) + 1.3333\delta \frac{\pi m_K}{\sqrt{2}\bar{m}} (D^2 - 3F^2), \\ Y_{\text{full}} &= 1 - 0.4125 \frac{m_K^3}{8\pi\bar{m}f_\pi^2} (D^2 - 3F^2). \end{aligned} \quad (56)$$

(The parameter γ drops out of this particular combination and we again take $\alpha = 0$.) These quantities still depend on the other bare parameters, D , F and \bar{m} . Again, they could be different in the quenched and full theories, and I will leave the quenched values as free parameters. Substituting $m_K = 495 \text{ MeV}$, $f_\pi = 132 \text{ MeV}$, $D_{\text{full}} = 0.75$, $F_{\text{full}} = 0.5$ and $\bar{m}_{\text{full}} = 1 \text{ GeV}$ [25] finally gives

$$\frac{Y_{\text{quenched}}}{Y_{\text{full}}} = 1 - 0.0214 + \left[0.293 \frac{\delta}{0.2} - 0.306 \right] \frac{(D^2 - 3F^2)_{\text{quenched}}}{\bar{m}_{\text{quenched}}/1 \text{ GeV}}. \quad (57)$$

For any reasonable values of \bar{m} and δ , and for $(D^2 - 3F^2)_{\text{quenched}}$ not too far from its full theory value of -0.1875 , the difference between the quenched and full theories as measured by the ratio $Y_{\text{quenched}}/Y_{\text{full}}$ is not more than a few percent. Of course the same comment that applied in the case of f_K/f_π applies here, that part of the difference may have been washed out by taking “ratios of ratios”. Summarizing, the conclusion of this analysis seems to be that the error from quenching for octet baryon masses is at least a few percent, and could be as much as 20%.

6. A sickness of quenched QCD

Let us again consider the quenched result for f_K/f_π , eq. (41), as a function of the quark masses (using treelevel relations between meson masses and quark masses),

$$\left(\frac{f_K}{f_\pi}\right)_{\text{quenched}}^{1\text{-loop}} = 1 + \frac{\mu^3/3}{16\pi^2 f_\pi^2} \left[\frac{m_u + m_s}{2(m_s - m_u)} \log \frac{m_s}{m_u} - 1 \right] + \hat{\text{L}} - \text{term.}$$

From this expression it is clear that we cannot take $m_u \rightarrow 0$ keeping m_s fixed, or, to put it differently, that if we take both m_u and m_s to zero keeping the ratio fixed, the limit depends on this ratio, and is not equal to one! This is quite unlike the case of full ChPT, where one can take any quark mass to zero uniformly, and deviations from $SU(3)$ symmetry due to this quark mass vanish in this limit. Technically, the reason for this strange behavior is that there is another mass μ , which, as we argued before, cannot be avoided in quenched ChPT. This mass is related to the singlet part of the η' mass, and is not a free parameter of (quenched) QCD. Even if we do not consider any Green's functions with η' external lines, this mass shows up through the double pole term in eq. (39) on internal lines. Because of the double pole, such contributions can lead to new infrared divergences in the $m_\pi \rightarrow 0$ limit. This problem with the chiral limit of quenched ChPT shows up in other quantities, such as meson masses and $\langle \bar{\psi}\psi \rangle$ [6,7].

A question one might ask is whether this problem is an artifact of one loop quenched ChPT [8]. For instance, if we would sum all contributions to the η' propagator, maybe the double pole term would become softer in the $p \rightarrow 0$ limit, improving the infrared behavior of diagrams in which the double pole terms appear. Let us address this question in the chiral limit, $m_a = 0$, where the problem is most severe. In the full theory, we can write the fully dressed η' propagator as

$$\frac{Z(p)}{p^2 + \Sigma(p)}, \quad (58)$$

and define $\mu_F^2(p) = \Sigma(p)$, which onshell is the η' mass in the chiral limit. Likewise, in the

quenched theory we can write the dressed η' , $\tilde{\eta}'$ propagator as

$$Z_Q(p) \left[\frac{1}{p^2} \begin{pmatrix} 1 & 0 \\ 0 & -1 \end{pmatrix} - \frac{\mu_Q^2(p)}{(p^2)^2} \begin{pmatrix} 1 & 1 \\ 1 & 1 \end{pmatrix} \right], \quad (59)$$

which defines $\mu_Q^2(p)$. To leading order in $1/N_c$, these two definitions of $\mu^2(p)$ should lead to the same result:

$$\mu_Q^2(p) = \mu_F^2(p) \left(1 + O\left(\frac{1}{N_c}\right) \right).$$

We also believe that $\mu_F^2(p=0)$ is not equal to zero, since we expect the η' in the full theory to remain a well-behaved, massive particle in the chiral limit. This implies, insofar as we can rely on the large N_c expansion, that $\mu_Q^2(0) \neq 0$, and that the double pole in eq. (39) is a true feature of the theory. (The argument can be repeated at nonzero quark masses, which is necessary if the chiral limit of quenched QCD does not exist.)

While this argument is not very rigorous, I believe that the foregoing discussion implies that the chiral limit of quenched QCD really does not exist. This belief is furthermore supported by the following remarks:

- Sharpe [7] has summed a class of diagrams in the case of degenerate quark masses for a very simple quantity (the pion mass), and found a result that is actually more divergent than the one loop result.
- With nondegenerate quark masses there are many more diagrams that are infrared divergent in the chiral limit, and it is even less probable that resummation will improve the situation.
- Any mechanism improving the infrared behavior would have to work for each divergent quantity. One expects that such a mechanism would be related to the double pole term in the η' propagator, which created the problem in the first place. But this seems unlikely in view of the arguments given above.
- The bare quark mass parameter appearing in the chiral effective action is not the same as that appearing in the (unrenormalized) QCD lagrangian. But one can argue that the

two bare quark masses should be analytically related, and the infrared problem is not just a problem of quenched ChPT, but of quenched QCD.

7. Conclusion

The quenched approximation leads to an unknown systematic error in all lattice calculations that employ this approximation. It would of course be very nice to have a parameter that interpolates between full and quenched QCD, and in principle the quark masses could play such a role, since one expects that quenched QCD corresponds to full QCD with very heavy quarks. One would have to distinguish here between valence and sea quark masses, and it is the sea quark mass that would play the role of such a parameter. This distinction can indeed be made by considering so-called partially quenched theories [28], but no practical scheme to implement this idea is known.

Quenched QCD can be defined from a euclidean pathintegral as rigorously as full QCD. In this talk I have explained that euclidean quenched ChPT can be used as a tool for a systematic investigation of quenched QCD. Quenched ChPT does not quite accomplish a task equivalent to that of an interpolating parameter. Since the bare parameters appearing in the quenched and full chiral effective actions are not the same (as explained in section 5) one cannot directly compare quantities calculated in full and in quenched ChPT. However, one can calculate combinations of physical quantities which do not depend on the bare parameters, and in that case a direct comparison between quenched and full QCD is possible, as we demonstrated with an example involving meson decay constants. This makes it possible to estimate lower bounds on the differences which come from quenching; these estimates are dependent on the values of the meson masses, which can be taken to be the (known) independent parameters of the theory. For realistic values of these masses, such differences turn out to be of the order of a few percent for ratios of decay constants

and for baryon octet splittings.

The disadvantage of this more conservative approach is that part of the difference maybe hidden, because these specific combinations of physical quantities maybe less sensitive to the effects of quenching than other quantities of interest. This is particularly clear in the example of baryon octet masses. In this case, a comparison based on the assumption that the bare parameters of the full and quenched effective theories are the same, lead to differences of up to 20% and more. Of course, it is not known to what extend this assumption is valid.

The differences between the quenched and full theories become markedly larger for decreasing quark masses. This is due to the fact that new infrared divergences occur in quenched QCD, which do not have a counterpart in full QCD. These divergences lead to the nonexistence of the chiral limit for quenched ChPT (as discussed in section 6). The origin of this phenomenon can be traced to the special role of the η' in the quenched approximation. In the quenched approximation, the η' is a Goldstone boson (it develops massless poles in the chiral limit), but an additional double pole term arises in its propagator, rendering it a “sick” particle. For nondegenerate quark masses this problem is also inherited by the π^0 and the η . In section 6 I argued that the nonexistence of the chiral limit is a fundamental feature of quenched QCD.

In principle therefore, the chiral expansion breaks down for quenched QCD. For very small quark masses, at fixed values of the singlet part of the η' mass μ^2 , the expansion becomes unreliable. In order to make progress, one may take the expansion to be an expansion in $\mu^2/3$ (which was shown to be roughly equal to m_K^2 phenomenologically), with coefficients which are functions of the quark mass. These functions sometimes show divergent behavior in the chiral limit (*e.g.* the one loop correction to f_K/f_π). If such divergences occur, the expansion is only valid for a range of quark masses which are neither too small, nor too large. It would be interesting to see whether this point of view can be made solid. One

way to check whether quenched ChPT makes any sense, is to compare its predictions with numerical results. Results for f_K/f_π (section 5) and B_V (section 3) are consistent with one loop quenched ChPT.

It is in principle interesting to study any quantity which is being computed in quenched lattice QCD in ChPT, for those quantities for which ChPT is applicable (meson masses, decay constants, condensates and the kaon B parameter have been calculated [6,5,8]). As discussed, this includes not only Goldstone meson physics *per se*, but also chiral corrections to baryon masses [11], and for the same reason, to mesons containing heavy quarks.

Recently, also attempts have been made to compute pion and nucleon scattering lengths [29,30] from quenched lattice QCD. If one tries to calculate the $I = 0$ pion scattering amplitude in quenched ChPT, one actually finds that the imaginary part is divergent at threshold, even for nonvanishing pion mass [31]! Again, this can be related to double pole terms in the η' propagator. Apparently euclidean quenched correlation functions in general cannot be analytically continued to Minkowski space-time. (The euclidean four pion correlation functions are well defined.) Further work is needed on pion scattering lengths.

Acknowledgments

First, I would like to thank Claude Bernard for a pleasant collaboration, and for very many discussions. I also thank Steve Sharpe, Jim Labrenz, Akira Ukawa, Hari Dass, Rajan Gupta, Julius Kuti and Don Weingarten for discussions. I am grateful for the opportunity to present these lectures given to me by the organizers of the XXXIV Cracow School of Theoretical Physics, Zakopane, Poland. This work is supported in part by the Department of Energy under contract #DOE-2FG02-91ER40628.

REFERENCES

1. S.R. Sharpe, in *The Fermilab Meeting*, 7th meeting of the DPF, eds. C.H. Albright, P.H. Kasper, R. Raja and J. Yoh, World Scientific, 1993.
2. P.B. Mackenzie, in AIP conference proceedings 302 (XVIth International Symposium on Lepton and Photon Interactions), eds. P. Drell and D. Rubin, 1994; A.S. Kronfeld and P.B. Mackenzie, *Ann. Rev. Nucl. Part. Phys.* **43** (1993) 793.
3. Lattice'93, proceedings of the International Symposium on Lattice Field Theory, Dallas, Texas, 1993, published as *Nucl. Phys. B (Proc.Suppl.)* **34** (1994).
4. H. Hamber and G. Parisi, *Phys. Rev. Lett.* **47** (1981) 1792; E. Marinari, G. Parisi and C. Rebbi, *Phys. Rev. Lett.* **47** (1981) 1795; D.H. Weingarten, *Phys. Lett.* **109B** (1982) 57.
5. S.R. Sharpe, *Phys. Rev.* **D41** (1990) 3233; *Nucl. Phys. B (Proc.Suppl.)* **17** (1990) 146; G. Kilcup *et al.*, *Phys. Rev. Lett.* **64** (1990) 25; S.R. Sharpe, DOE/ER/40614-5, to be published in *Standard Model, Hadron Phenomenology and Weak Decays on the Lattice*, ed. G. Martinelli, World Scientific.
6. C.W. Bernard and M.F.L. Golterman, *Phys. Rev.* **D46** (1992) 853; *Nucl. Phys. B (Proc.Suppl.)* **26** (1992) 360.
7. S.R. Sharpe, *Phys. Rev.* **D46** (1992) 3146; *Nucl. Phys. B(Proc.Suppl.)* **30** (1993) 213.
8. C.W. Bernard and M.F.L. Golterman, *Nucl. Phys. B(Proc.Suppl.)* **30** (1993) 217.
9. J. Gasser and H. Leutwyler, *Phys. Lett.* **184B** (1987) 83, *Phys. Lett.* **188B** (1987) 477, and *Nucl. Phys. B307* (1988) 763; H. Leutwyler, *Nucl. Phys. B (Proc.Suppl.)*

- 4 (1988) 248 and Phys. Lett. **189B** (1987) 197; H. Neuberger, Nucl. Phys. **B300** (1988) 180; P. Hasenfratz and H. Leutwyler, Nucl. Phys. **B343** (1990) 241.
10. R. Gupta, to be published in the proceedings of the International Symposium on Lattice Field Theory, Bielefeld, Germany, 1994.
 11. J.N. Labrenz and S.R. Sharpe, Nucl. Phys. **B** (Proc.Suppl.) **34** (1994) 335.
 12. S. Weinberg, Physica **96A** (1979) 327.
 13. H. Georgi, *Weak Interactions and Modern Particle Physics*, Benjamin, 1984.
 14. J. Gasser and H. Leutwyler, Nucl. Phys. **B250** (1985) 465.
 15. S. Weinberg, Phys. Rev. 166 (1968) 1568; S. Coleman, J. Wess and B. Zumino, Phys. Rev. 177 (1969) 2239; C.G. Callan, S. Coleman, J. Wess and B. Zumino, Phys. Rev. 177 (1969) 2247.
 16. G. 't Hooft, Phys. Rev. Lett. **37** (1976) 8.
 17. E. Witten, Nucl. Phys. **B156** (1979) 269; G. Veneziano, Nucl. Phys. **B159** (1979) 213.
 18. C.W. Bernard, in *From Actions to Answers*, proceedings of the 1989 TASI School, eds. T. DeGrand and D. Toussaint, World Scientific, 1990.
 19. J. Bijnens, H. Sonoda and M. Wise, Phys. Rev. Lett. **53** (1985) 2367.
 20. P. Langacker and H. Pagels, Phys. Rev. **D8** (1973) 4595.
 21. A. Morel, J. Physique **48** (1987) 111.
 22. For a description of the properties of graded groups, see for example, B. DeWitt, *Supermanifolds*, Cambridge, 1984.

23. Y. Kuramashi, M. Fukugita, H. Mino, M. Okawa and A. Ukawa, Phys. Rev. Lett. **72** (1994) 3448; Nucl. Phys. **B** (Proc.Suppl.) **34** (1994) 117.
24. E. Jenkins and A. Manohar, Phys. Lett. **255B** (1991) 558; E. Jenkins, Nucl. Phys. **B368** (1992) 190.
25. V. Bernard, N. Kaiser and U. Meissner, Z. Phys. **C60** (1993) 111.
26. T. Hatsuda, Nucl. Phys. **B329** (1990) 376; S.R. Sharpe, private communication.
27. F. Butler, H. Chen, J. Sexton, A. Vaccarino and D. Weingarten, Phys. Rev. Lett. **70** (1993) 2849; Nucl. Phys. **B** (Proc.Suppl.) **30** (1993) 377.
28. C.W. Bernard and M.F.L. Golterman, Phys. Rev. **D49** (1994) 486; Nucl. Phys. **B** (Proc.Suppl.) **34** (1994) 331.
29. R. Gupta, A. Patel and S.R. Sharpe, Phys. Rev. **D48** (1993) 388.
30. Y. Kuramashi, M. Fukugita, H. Mino, M. Okawa and A. Ukawa, Phys. Rev. Lett. **71** (1993) 2387.
31. C.W. Bernard, M.F.L. Golterman, J.N. Labrenz, S.R. Sharpe and A. Ukawa, Nucl. Phys. **B** (Proc.Suppl.) **34** (1994) 334.

This figure "fig1-1.png" is available in "png" format from:

<http://arxiv.org/ps/hep-lat/9411005v1>